



## Bimodality and negative heat capacity in multifragmentation

B. Tamain, R. Bougault, O. Lopez, M. Pichon

### ► To cite this version:

B. Tamain, R. Bougault, O. Lopez, M. Pichon. Bimodality and negative heat capacity in multifragmentation. International Workshop on Multifragmentation and Related Topics (IWM2003), Nov 2003, CAEN, France. pp.83-88. in2p3-00023919

**HAL Id: in2p3-00023919**

**<https://hal.in2p3.fr/in2p3-00023919>**

Submitted on 24 Mar 2005

**HAL** is a multi-disciplinary open access archive for the deposit and dissemination of scientific research documents, whether they are published or not. The documents may come from teaching and research institutions in France or abroad, or from public or private research centers.

L'archive ouverte pluridisciplinaire **HAL**, est destinée au dépôt et à la diffusion de documents scientifiques de niveau recherche, publiés ou non, émanant des établissements d'enseignement et de recherche français ou étrangers, des laboratoires publics ou privés.

# Bimodality and negative heat capacity in multifragmentation

B. Tamain, R. Bougault, O. Lopez, M. Pichon for the INDRA and ALADIN collaborations

LPC-ENSICAen and University, 14050 Caen cedex, France

## Abstract

This contribution addresses the question of the possible link between multifragmentation and the liquid-gas phase transition of nuclear matter. Bimodality seems to be a robust signal of this link in the sense that theoretical calculations indicate that it is preserved even if a sizeable fraction of the available energy has not been shared among all the degrees of freedom. The corresponding measured properties are coherent with what is expected in a liquid-gas phase transition picture. Moreover, bimodality and negative heat capacity are observed for the same set of events.

## 1 BIMODALITY : A ROBUST SIGNAL

Bimodality is expected if a system explores a first order phase transition at a given temperature. This prediction is obtained for instance from lattice-gas calculations in which the order parameter is the size  $A_{big}$  of the heaviest fragment. The corresponding observation probability is plotted in the first three pictures of figure 1 [1,2] for three temperatures of the system, below, at, and above the transition one.  $A_{big}$  has been normalized to the size of the whole system (216 interacting particles).

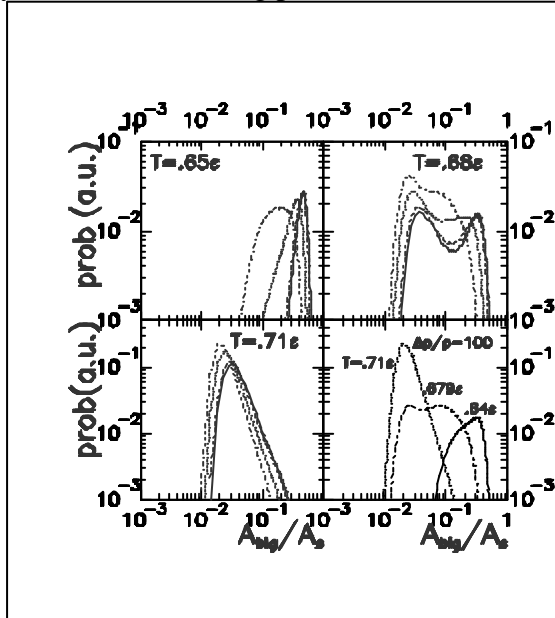


Figure 1: Results of a lattice gas calculation for a system of 216 particles at three temperatures indicated in the plots. Various curves correspond to full equilibrium (solid lines in the first three pictures) and to increasing memory of the entrance channel (see text).

Bimodality is clearly observed at the transition temperature if full thermal equilibrium is achieved (solid lines in the 3 first plots). The dashed lines correspond to a situation of incomplete equilibrium : a percentage of linear momentum aligned on a given (beam) axis simulates the memory of the entrance channel. The aligned additional momentum which is 10% (dashed), 50% (dotted), and 100% (dotted-dashed) in the 3 first plots does not destroy the bimodality signal even if half of the initial momentum is kept aligned along the beam direction. This feature is clearly seen in the last plot showing in the 100% case the distributions for the three temperature values around the transition one. This means that bimodality is a robust signal of a first order phase transition even in a non-equilibrated (collision) process.

## 2 BIMODALITY FROM EXPERIMENT

In order to select from data a situation equivalent to a canonical one, we have studied bimodality for a quasiprojectile (QP) released in a binary collision. Au + Au and Xe + Sn symmetrical systems have been studied from 60 to 100 MeV/u by setting the Indra detector at GSI (Indra-Aladin collaboration). The sorting has been obtained from the transverse energy  $E_{trans}$  of light particles ( $Z = 1$  and  $2$ ) on the quasitarget (QT) side. This quantity reflects the temperature of the (small) heat bath (QT) if equilibrium is achieved. In any case it measures the violence of the collision. Moreover, it ensures a complete decorrelation (but physical) between

sorting particles (QT side) and QP decay properties. We have tested from invariant cross section plots that the collisions of interest in this paper are really binary with a weak influence of midrapidity emission (see section 3). The two sources are well-resolved thanks to their large relative velocities in the incident energy range.

We have used two variables as order parameters: the largest fragment size  $Z_{max}$ , and the asymmetry of the two largest fragments:  $varsym = (Z_{max} - Z_{max-1}) / (Z_{max} + Z_{max-1})$  where  $Z_{max-1}$  is the charge of the second heaviest fragment. In order to avoid spurious effects due to the lost of a heavy fragment by the detection set up, we asked for a total QP charge (forward hemisphere in the center of mass system) of at least 80% of the initial projectile charge. No other cuts have been performed. Fission events for the Au + Au system were easily recognized. The corresponding fragments have been put together to reconstruct the initial nucleus before decay. The procedure was justified by the fact that fission happens at normal density and has nothing to do with multifragmentation which is expected to take place at low density if it is linked with the phase transition.

## 2.1 General behavior

Bimodality may be recognized without any sorting as it is shown in the example of the 100 MeV/u Au+Au system (figure 2).

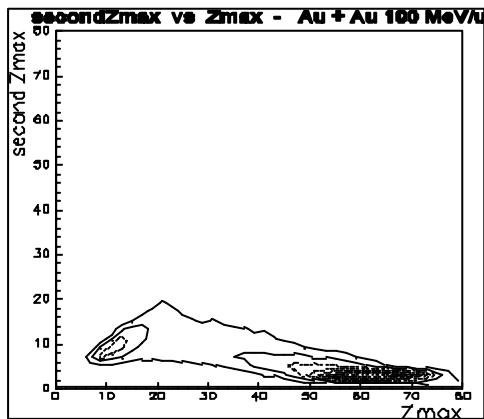


Figure 2 : correlation  $Z_{max-1}$  versus  $Z_{max}$  for the 100 MeV/u Au+Au system ; no sorting.

Figure 3 refers to the correlation between  $varsym$  and  $Z_{max}$  after sorting by using the transverse energy

$E_{trans}$  on the QT side. The corresponding distribution (last plot in figure 3) has been divided in 8 zones for which the correlations are shown from the most peripheral collisions (upper left) to the most central ones.

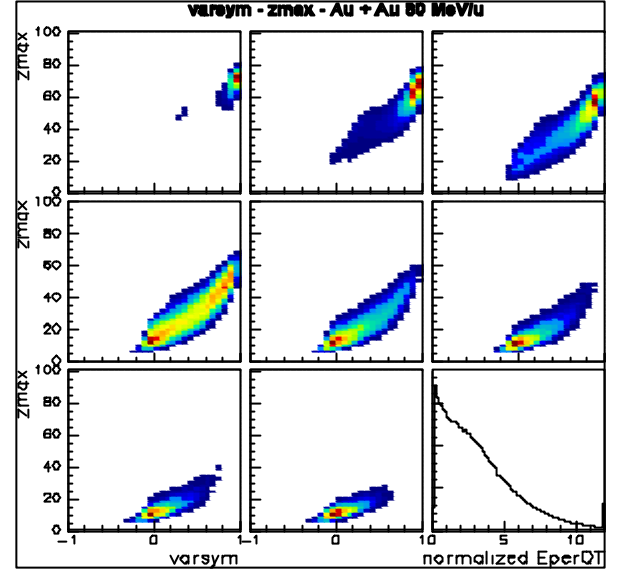


Figure 3 :  $varsym - Z_{max}$  plots for various  $E_{trans}$  bins for the 80 MeV/u Au+Au system. Last plot:  $E_{trans}$  distribution.

In the fourth zone, one jumps from residue-like events (large  $Z_{max}$  and large  $varsym$ ) to multifragment events (small  $Z_{max}$  and  $varsym$ ). This feature is also visible on the projection on the abscissa axis (figure 4): bimodality is observed. It is the case for the 6 studied systems.

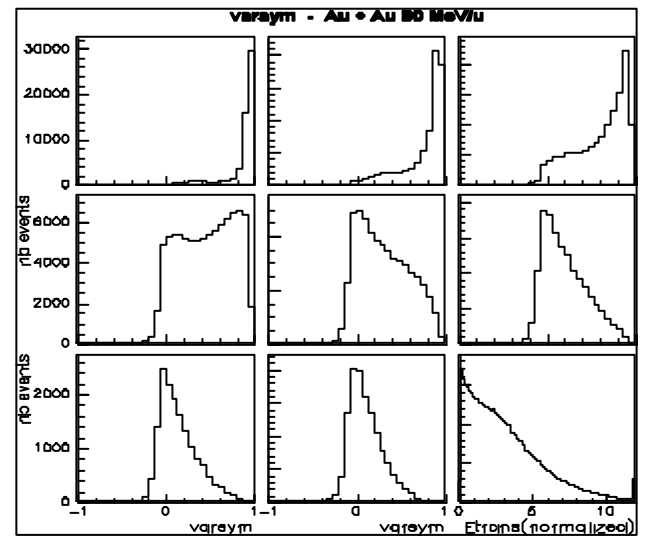


Figure 4 :  $varsym$  distributions (projections of figure 3) for the 8  $E_{trans}$  bins. Last plot:  $E_{trans}$  distribution.

It has been shown that the  $E_{trans}$  value per nucleon for which one observes the transition is the same for the Xe + Sn and Au + Au systems at a given beam energy per nucleon. This result is expected if the transition happens at a given temperature. However, for a selected projectile-target system, the transition value of the transverse energy increases with the bombarding energy (from 256 to 425 MeV for the Au + Au system when the beam energy rises from 60 to 100 MeV/u). This increase is probably due to the growing importance of preequilibrium emission at large bombarding energies.

## 2.2 Towards thermalized events selection

Dynamical effects can be easily recognized in many aspects of nucleus-nucleus collisions. One of them is the fact that fragment emission in the QP frame is not isotropic [3]. The heaviest decay product is rather often forward emitted : its emission angle  $\theta$  has the memory of the beam direction. Most but not all events behave this way. This means that it is possible to select events for which the entrance channel memory effect is larger or weaker.

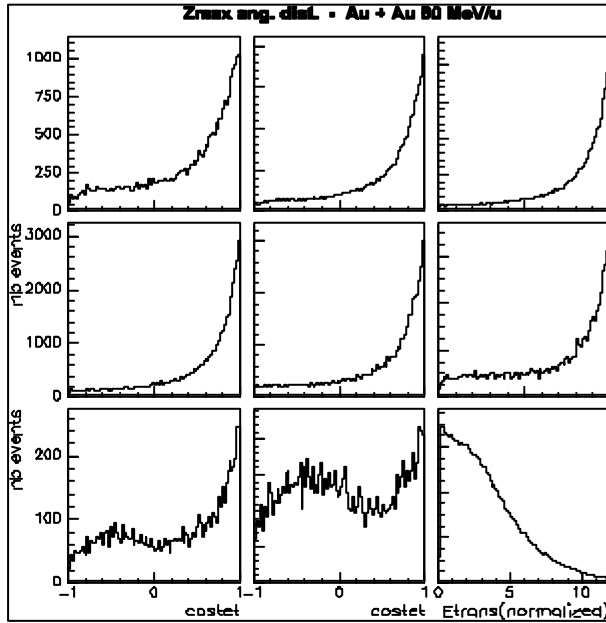


Figure 5 : Angular distributions of the heaviest QP decay product in the QP frame for various QT  $E_{trans}$  bins. The heaviest fragment is mostly forward emitted. The  $E_{trans}$  distribution shown in the last bin corresponds to events with at least 2 IMF attributed to the QP.

A typical result is shown in figure 5 in which the heaviest QP fragment  $\cos(\theta)$  distribution may be used to select events with more (forward emission) or less (backward emission) memory of the entrance channel beam direction.  $\theta$  has been calculated in the QP frame. The QP velocity has been reconstructed from the total linear momentum carried out by IMF emitted from the QP (forward emission in the cm system). In figure 6, the plots are similar to figure 4 ones but events with  $\cos(\theta)$  lower than -0.4 have been selected. It turns out that the bimodality picture is much better evidenced from this figure which corresponds to more thermalized events. This result is coherent with the predictions of figure 1. Moreover, bimodality is observed for smaller  $E_{trans}$  values (in bin 3 rather than in 4th bin) which is coherent with a selection of events with a better energy relaxation.

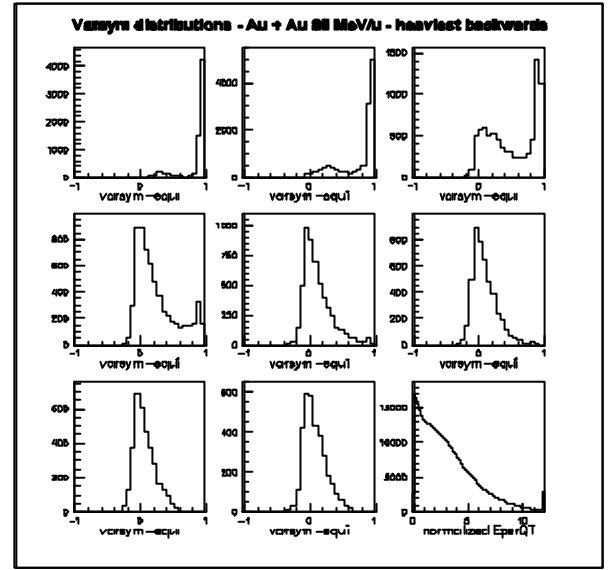


Figure 6 : similar to figure 4 but for events in which the largest QP fragment has been backward emitted (see text)

## 2.3 Excitation energy distributions

It is possible to perform calorimetry for events with low (resp. high)  $varsym$  values ( $varsym < 0.3$  - resp.  $> 0.7$ ). The corresponding results are shown in figure 7. The events are again sorted according to QT  $E_{trans}$ . No selection has been achieved from the  $\cos(\theta)$  distributions. It turns out that the events with large  $varsym$  values (residue like) correspond to a mean excitation energy value, which is lower than the mean value for small

*varsym* (multifragment emission) events. This result is also expected in a bimodality picture linked with a liquid-gas phase transition at the transition temperature. Moreover, one may notice that the excitation energy values around which bimodality takes place (fourth bin for which both classes of events are about equally probable) is around 6 MeV/u, i.e. in the excitation energy range which is expected for this transition.

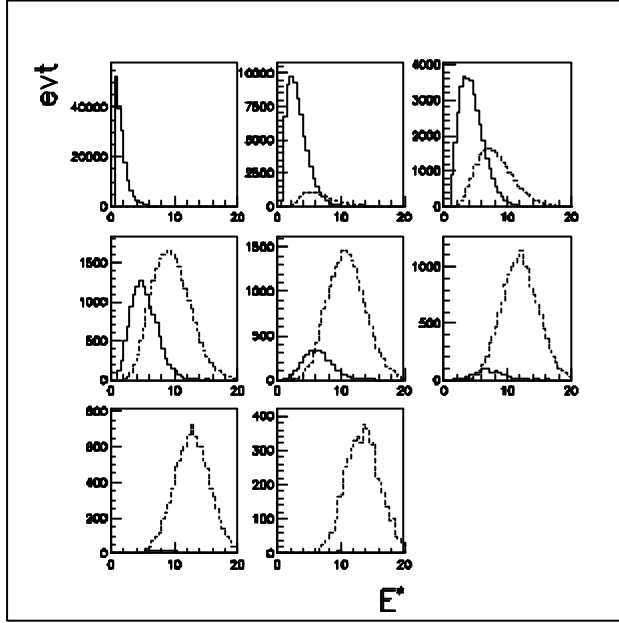


Figure 7 : Excitation energy distributions for large (solid lines) and low (dashed lines) *varsym* values (resp.  $>0.7$  and  $<0.3$ ). Events have been sorted according to the QT  $E_{trans}$  distribution as in figure 3. Mean excitation energies are larger for multifragmentation events. Au + Au system at 80 MeV/u.

## 2.4 About a possible mechanism change

The experimental fact noticed in figures 3,4,6 is the sudden change of event topology when the violence of the collision becomes stronger. This feature can reflect a liquid-gas phase transition, but one may also argue about a possible mechanism change for intermediate impact parameters. More precisely one has to remember that neck-emission becomes significant for semiperipheral collisions. In such cases, the assumption of a binary-like process for which it is possible to separate QP from QT contributions can be questionable.

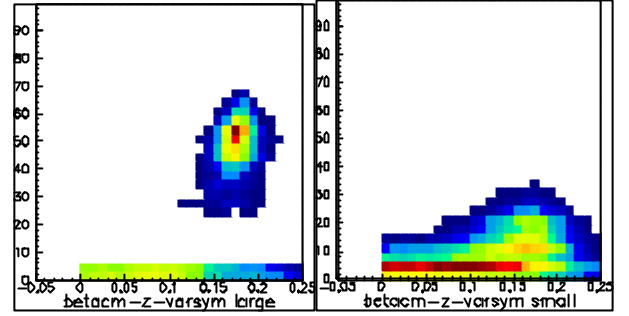


Figure 8 : Charge versus cm velocity (in c unit) for events of the fourth plot of figure 3 (bimodality transition region). Left (resp. right) side: selection of events with *varsym* larger than 0.8 (resp. lower than 0.2). All QP fragments with  $Z$  larger than 3 are involved in the picture.

In order to estimate the influence of mid-rapidity collisions, we have looked at the topology of events in the bimodality transition region (fourth plot in figure 3). In figure 8, we have distinguished residue-like events (*varsym* larger than 0.8 in the fourth plot of figure 3) from the multifragmentation events (*varsym* lower than 0.2). For all QP fragments ( $Z > 3$ ), one has plotted the correlation between the charge (ordinate) and the cm velocity (abscissa). It turns out that the intermediate velocity contribution (around zero velocity) is negligible or weak in both plots : for both classes of events, a QP can be defined and reconstructed with a small error. This behavior is confirmed from figure 9 which shows the cumulated charge density as a function of the cm velocity for both classes of events : the mid-rapidity emission does not exist for residue-like events and does not play a major role for multifragmentation ones.

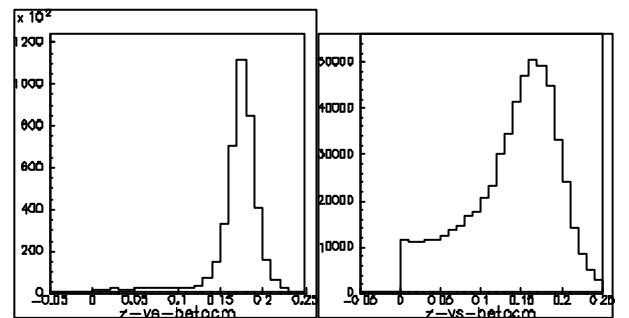


Figure 9 : Cumulated charge density for the events of figure 8 as a function of the cm velocity. Residue-like events (left plots of figures 8 and 9) are pure QP events. Multifragment-events (right side) correspond to QP decay with a small contribution of mid-rapidity emission.

This "pure" QP decay behavior is even better evidenced if one select events for which the heaviest QP fragment is backward emitted as in figure 6 selection. This is shown in figure 10 for the events in the bimodality transition bin: mid-rapidity emission is weaker than in figure 9 for multifragmentation events.

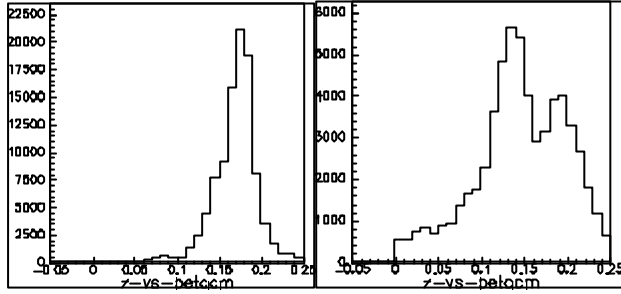


Figure 10 : Cumulated charge density (as in figure 9) for events for which the heaviest QP decay fragment has been backward emitted in the bimodality transition region (the left peak in the right plot is due to the heaviest fragment). The mid-rapidity emission is weaker than in figure 9 for multifragmentation events.

These observations are coherent with the interpretation of bimodality in terms of liquid-gas phase transition even if it is difficult to establish unambiguously this statement.

### 3 BIMODALITY AND HEAT CAPACITY

A possible further signal of phase transition is the negative heat capacity. It has been observed both in central [4] and peripheral [5] collisions involving nuclei in the gold region. We have hence tried to check to which extent the bimodality feature and the negative heat capacity signals may be correlated. For that purpose, we have sorted the events according to the QT  $E_{trans}$  bins used for the bimodality analysis (see figure 2). For each  $E_{trans}$  bins, one has obtained on an event by event basis the QP excitation energy (calorimetry method). To prevent from mid-rapidity contribution, calorimetry has been performed by using all IMF and only LCP emitted in the forward hemisphere of the QP frame. The QP velocity has been reconstructed from the IMF forward emitted in the center of mass system. The calculated LCP contribution has been

doubled to account for backward emitted particles and a neutron contribution has been included.

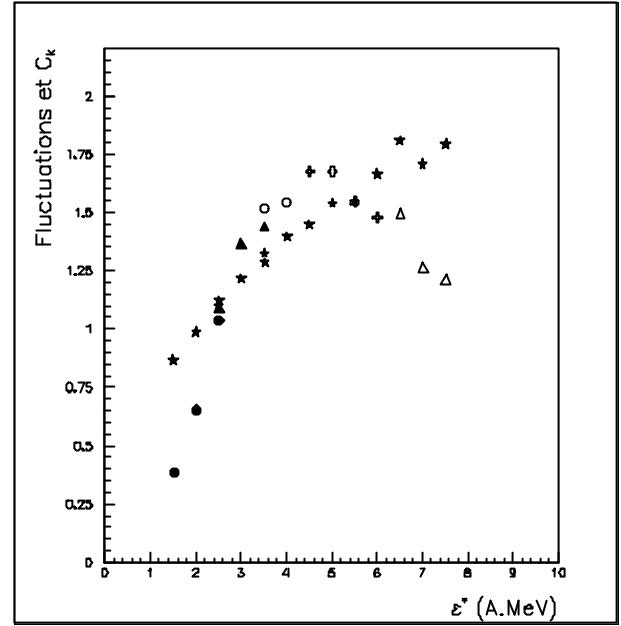


Figure 11 : The negative heat capacity signal corresponds to the situation where fluctuations in the sharing of the available energy between two classes of degree of freedom are larger than the canonical expectation. Both values are compared in this picture for various selections ( $E_{trans}$  bins). See text.

For each  $E_{trans}$  bins, one has obtained an excitation energy distribution. Only events around the mean value of the excitation energy distribution have been retained. A given symbol in figure 11 is associated with the corresponding involved excitation energies (abscissa). For instance, the 3 black dots correspond to the first  $E_{trans}$  bin of figure 2. Two quantities have been plotted in ordinate which are related to the fluctuations in the sharing of the available energy between potential and kinetic parts [4]. The stars are the expectation values in the canonical sharing. The other symbols correspond to experimental results for various  $E_{trans}$  bins. Open points correspond to the third bin of figure 2 and crosses to the fourth one. It turns out that the measured values exceed the expected canonical ones (negative heat capacity behavior) for these two  $E_{trans}$  bins. If one remembers that bimodality is observed (figure 2) for the 4<sup>th</sup> bin, one may conclude that both signals are coherent one with the other.

One has however to add the following information: the negative heat capacity signal observed from figure 11 is obtained only if one selects compact QP events, i.e. events for which the relative velocity between the heaviest QP fragment and the center of mass of the lighter ones is compatible with a coulomb repulsion. In other words the negative heat capacity is obtained if one eliminates events for which a significant memory of the entrance channel is obtained. Moreover, it is necessary either to eliminate QP fission decay events or to reconstruct the primary residue before fission. These necessary selections indicate that the negative heat capacity signal is less robust than bimodality: it is destroyed or at least attenuated if a significant proportion of the available energy is still stored along the beam axis.

## 4 CONCLUSIONS

We have seen in this contribution that bimodality is observed in peripheral nucleus-nucleus collisions for symmetrical medium mass (Xe + Sn) and large mass (Au + Au) systems between 60 and 100 MeV/u. This experimental feature has been evidenced in an analysis in which there is no spurious experimental effect since the sorting has been achieved on the QT side whereas the observation was focussed on the QP side. Bimodality is better exhausted if one select events for which the energy relaxation is better achieved. In the region where bimodality is observed, the excitation energy distribution is also bimodal, larger excitation energies being associated with the multifragmentation channel. It has been also established that bimodality and negative heat capacity signals are observed for similar sets of data provided one eliminates elongated QP decay events in the negative heat capacity analysis. These results are coherent with what is expected if a phase transition of the liquid-gas type takes place. It is however not fully established that these signals are convincing signatures of the occurrence of such a first order liquid-gas phase transition. To progress in this way, it is necessary to study other signals. One has for instance to correlate the signals

discussed in this paper with the delta scaling [6]. One has also to check that both sets of events in the transition region (residue-like and multifragmentation) correspond to similar temperatures. These analysis are under way but the temperature measurements are not simple since the available thermometers exhibit limitations and drawbacks which are different for residue-like and multifragmentation events. For instance, the thermometer based on the shape of the kinetic energy spectra is not correct in the multifragmentation case whereas the double ration thermometer is not suited for residue events. Nevertheless one has to succeed since it is only the coherence between many disconnected signals which can convince that a phase transition has been identified.

## 5 REFERENCES

- [1] F. Gulminelli and Ph. Chomaz, ArXiv: nucl-th/020932.
- [2] Ph. Chomaz, F. gulminelli and V. Duflot, Phys. Rev. E64 (2001) 046114.
- [3] J. Colin and the Indra coll., Physical Review C67 (2003) 064603
- [4] M. d'Agostino et al., Nucl. Phys. A650 (1999) 329
- [5] N. Le Neindre et al., Proceed. of the XXXVIII Int. Wint. Meet. on Nuc. Phys., Bormio, 2000, p2004
- [6] J. Frankland et al, this conf, and R. Botet, and M. Ploszajczak, World Scientific Lectures Notes in Physics, vol 65, 2002